Changes-of-mind in the absence of new post-decision evidence

Nadim A. A. Atiya[1†], Arkady Zgonnikov[2†], Denis O'Hora*[2], KongFatt Wong-Lin*[1],

1 Intelligent Systems Research Centre, School of Computing, Engineering and Intelligent Systems, Ulster University, Magee Campus, Derry∼Londonderry, UK
2 School of Psychology, National University of Ireland Galway, Galway, Ireland

†These authors contributed equally to this work.
* Correspondence to: KongFatt Wong-Lin (k.wong-lin@ulster.ac.uk), Denis O'Hora (denis.ohora@nuigalway.ie)

Abstract

Many decisions we make are occasionally accompanied by a change-of-mind. While considered a hallmark of cognitive flexibility, the mechanism underlying change-of-mind behaviour remains elusive. Previous studies on perceptual decision making have focused on changes-of-mind that are primarily driven by the accumulation of additional noisy sensory evidence after the initial decision. In a motion discrimination task, we demonstrate that changes-of-mind can occur even in the absence of additional evidence after the initial decision. However, in contrast to previous studies on changes-of-mind, the majority of changes-of-mind in our experiment occurred in trials with prolonged initial response times. This suggests a distinct mechanism underlying such changes. Using a simplified version of our recently-developed neural circuit model of decision uncertainty and change-of-mind behaviour, we demonstrate that this phenomenon is associated with top-down signals mediated by an uncertainty-monitoring neural population. Such a mechanism is consistent with recent neurophysiological evidence showing a link between changes-of-mind and elevated top-down neural activity. Our model explains the long response times associated with changes-of-mind through high decision uncertainty levels in such trials, and readily accounts for the observed motor response trajectories. Overall, our work provides a computational framework that explains changes-of-mind in the absence of new post-decision evidence.

Authors Summary

We used limited availability of sensory evidence during a standard motion discrimination task, and we demonstrated that change-of-mind could occur after sensory information was no longer available. Unlike previous studies, our experiment further indicated that change-of-mind was strongly linked to slow response time. We used a simplified version of our previous neural computational model of decision uncertainty and change-of-mind to account for these experimental observations. Importantly, our model showed that the replication of these experimental results required a strong link between change-of-mind and high decision uncertainty (i.e. low decision confidence), reinforcing our previous work that links change-of-mind with decision uncertainty/confidence.

Introduction

Making perceptual decisions is ubiquitous in our daily lives, for instance, while driving in foggy conditions, or while attempting to visually spot an individual in the crowd. As these decisions vary in difficulty, so does our ability to make accurate and well-timed responses [1–3]. In some situations, an initial decision can be revised as new evidence arrives [4–8]. For instance, our interpretation of a road sign can change as we approach it, which sometimes results in a change-of-mind. Previous work investigating changes-of-mind has predominantly focused on revising a decision in response to new sensory evidence [4, 6, 7, 9]. Such studies demonstrated that the frequency of changes-of-mind increases with higher task difficulty, and that the majority of such changes improve the impending initial choices.

These behavioural findings were explained by cognitive models [4, 6] which extended the drift-diffusion model of decision making [10–12]. A central feature of these models is the temporal accumulation of noisy momentary evidence over time: when the accumulated evidence reaches a prescribed threshold, a choice is made. In extended drift-diffusion models (eDDM) [4, 6], evidence accumulation continues after the initial decision, which may lead to a change-of-mind if the accumulated evidence reaches a second prescribed threshold. Late-arriving sensory information, or any explicitly provided additional evidence [7], can feed into this extended accumulation process, thereby potentially reversing the initial decision. In many situations, however, additional post-decision evidence is not available and therefore cannot contribute to the revision of an initial decision. Moreover, it is not well understood whether the eDDM can readily account for situations where we reverse an initial decision in the absence of additional post-decision evidence. Thus, the mechanism underlying such changes-of-mind in the absence of additional post-decision evidence remains unclear [4, 13].

Recently, the neural correlates of change-of-mind behaviour in humans and primates have been gradually revealed [5, 7]. In particular, fMRI recordings indicated a strong correlation between changes-of-mind and increased activity in the prefrontal cortex [7]. This correlation supported the argument that top-down signals could play an important role in error correction mechanisms [14]. However, the neural mechanism by which these top-down signals lead to a change-of-mind has, so far, remained elusive. Furthermore, it is still unclear how this mechanism is linked to other metacognitive processes partially mediated by the frontal cortex, particularly, the encoding of decision uncertainty (or confidence) [15–17].

In this work, we investigate changes-of-mind in the absence of additional post-decision sensory evidence. In contrast to previous studies, the majority of changes-of-mind we observed were associated with prolonged initial response times. Using a neural circuit model, we demonstrate that these changes-of-mind can be attributed to neural feedback control mediated by decision uncertainty. This suggests that top-down uncertainty monitoring could play an important role in inducing changes-of-mind in the absence of additional post-decision evidence, which is consistent with recent neurophysiological evidence [7, 14].Overall, our work provides a computational framework that explains changes-of-mind in the absence of additional post-decision evidence, from the sensory integration stage up to the motor output.

Results

Cognitive task and neural circuit model

Four participants completed a perceptual decision-making task (2400 trials) in which, upon initiating a trial, a random dot kinematogram (RDK) stimulus [18, 19] appeared

Fig 1. Experimental setup and a schematic diagram of the neural circuit model. **(a)** Participants initiated a trial by clicking a start button at the bottom of the screen. After a short random delay (uniformly distributed over 700-1000ms), a random dot kinematogram appeared for 800ms. Participants then chose between two targets: Left or Right. Immediately after the choice, the feedback (red or green circle) was displayed for 300ms, followed by the fixation point (300ms). **(b)** Our neural circuit decision-making model consists of three modules. The sensorimotor module (blue box) consists of two mutually inhibitory (lines with filled circles) neuronal populations selective for Leftward/Rightward motion with recurrent excitation (curled black arrows). The uncertainty-monitoring population (red circle) receives summed input from the sensorimotor populations. 600ms after stimulus onset, the summed input is integrated and fed back to the sensorimotor populations (red arrow). The hand response module (green box) consists of two mutually inhibitory neuronal populations that integrate the output from the corresponding sensorimotor population. Model results in all subsequent figures were obtained via simulating the model using a single set of parameters (see Table 4 for parameter values).

after a random delay (uniformly distributed over 700-1000ms). The RDK stimulus was displayed for 800ms, followed by a choice prompt. Participants then decided whether the majority of the randomly moving dots were moving towards the right or the left. The participants were instructed to respond as quickly and accurately as possible by moving a computer mouse cursor to one of the two choice target locations in the top corners of the computer screen and clicking on it (Figure 1a). The difficulty of the task was varied via the *motion coherence* parameter, which controlled the probability of each dot moving in one direction (left or right, determined randomly in the beginning of the trial). In the vast majority of the trials, participants responded by moving the mouse cursor directly to a choice target. However, participants were free to reverse their initial decision before clicking on one of the choice targets, although they were not explicitly instructed that this is possible. This resulted in 294 change-of-mind trials (3% of all trials), in which participants reversed the initial decision.

To shed light on the potential mechanism underlying the observed changes-of-mind, we simulated and analyzed a computational model of decision uncertainty and changes-of-mind that is built on our previous work [20] (Figure 1b). The previous model consists of an inhibitory neuronal population receiving summed stimulus input from the sensorimotor populations. This inhibitory population in turn inhibits a neighbouring excitatory uncertainty-encoding population, which also receives tonic excitatory input. Finally, as long as the response is not initiated (i.e. response threshold for the activity of the sensorimotor population has not been reached), the sensorimotor populations receive equal excitatory feedback from the uncertainty-encoding population.

This cortical circuit model was previously shown to account for decision uncertainty and change-of-mind behaviour reported in previous work [4, 8, 17, 21], while capturing recent neurophysiological evidence of encoding decision confidence [7, 14, 17]. Here, we propose a more simplified neural circuit architecture. Specifically, we use only one neuronal population to encode uncertainty, termed the *uncertainty-monitoring population* (Figure 1b). While less neurally plausible (i.e. not reminiscent of a cortical column), the model could still replicate the main results in [20] with appropriate parameter changes (see Supplementary Figs. 2a and 2b). Below we shall demonstrate that this model qualitatively accounts for the observed change-of-mind behaviour.

Fig 2. Motor output of a decision. Top panels: representative mouse cursor trajectories from the experimental data in the x-y plane. Bottom panels: experimental mouse cursor trajectories in the x positional space (grey lines with markers) and model-generated motor output (blue solid lines). Participants reached one of the two choice targets (red/green areas) directly in non-change-of-mind trials (left), or after reaching towards the opposite target first in change-of-mind trials (right). See Methods for details on the linear mapping of the firing rates of the model hand response populations onto the x positional space.

Table 1. Parameters of a linear mixed-effects model analysing choice accuracy as a function of coherence, presence or absence of a change-of-mind, and trial number. The model included random intercept and random slope for coherence.

	Estimate	Std. Error	z value	Pr(>|z|)
Intercept	1.1432	0.2486	4.5984	0.0000
Coherence	7.0130	1.5219	4.6080	0.0000
Is CoM	-1.0372	0.2547	-4.0729	0.0000
Trial number	0.0491	0.0279	1.7587	0.0786
Coherence by Is CoM	-4.3762	1.9690	-2.2225	0.0262

Changes-of-mind can occur in the absence of post-decision sensory evidence

First, we investigated the motor response trajectories from our experimental data (Figure 2). In the case of trials without a change-of-mind, participants moved the mouse cursor directly towards a choice target. In change-of-mind trials, participants initially moved the mouse cursor towards one choice target, but then changed the movement direction to reach the opposite choice target instead.

In our computational model, we mapped the output of the neural activity of the motor populations (Figure 1b, blue box) onto the horizontal positional space alongside the mouse cursor trajectories from our experimental data (see Methods). We found that the model could produce motor response trajectories (along the horizontal line) that are qualitatively similar to the experimental ones (Figure 2, bottom panels).

Similar to previously-studied paradigms [4, 6, 9, 22], we observed changes-of-mind in a small proportion of trials (3%). However, these studies investigated changes-of-mind in situations where the response onset coincided with the stimulus offset [4, 23]. In such situations, late-arriving evidence (i.e. due to processing delays) could prompt a reconsideration of the initial decision (i.e. if the late-arriving evidence is in favour of the opposite choice). In contrast, in our paradigm, participants were instructed to respond only after stimulus offset, thereby limiting the potential effect of late-arriving evidence on changes-of-mind. Although in some trials the participants still started responding before stimulus offset, this behaviour was not associated with changes-of-mind (Supplementary Figure 1b). Specifically, early responses were observed only in three change-of-mind trials out of 294. Furthermore, 96% of all changes-of-mind in our experiment occurred later than 450ms after the initial response, suggesting that these changes-of-mind were not associated with delays in signal transduction and motor preparation [4, 24]. Taken together, these observations suggest that, in our experiment, changes-of-mind are not driven by late-arriving post-decision sensory evidence.

Fig 3. Performance in change-of-mind trials. **(a)** Overall probability of a change-of-mind sorted into error and correct changes from experimental data (left panel) and model simulations (right panel). Probability of a change-of-mind peaks at low-to-intermediate coherence levels, and decreases sharply at high coherence levels, with correct changes being more frequent than error changes at moderate to high coherence levels (0.128 and 0.256). **(b)** Psychometric function showing choice accuracy as a function of coherence level in the presence (grey) and absence (black) of a change-of-mind from the experiment (left panel) and the model (right). Accuracy generally increases as a function of coherence level, but is lower in change-of-mind trials (grey) compared to non-change-of-mind trials (black). However, for intermediate-to-high coherence levels (0.128 and 0.256), the accuracy of change-of-mind trials is above chance level (i.e. > 0.5). In both **(a)** and **(b)**, error bars indicate binomial proportion standard error of mean.

Changes-of-mind can lead to correction of impending errors in easy tasks

In change-of-mind trials, error-to-correct changes were more frequent than correct-to-error changes at 0.128 and 0.256 coherence levels (Figure 3a, left panel). In contrast, previous studies of changes-of-mind, supposedly caused by late-arriving evidence, have shown that error-to-correct changes were more likely than correct-to-error changes starting from the 0.064 coherence level [4,6]. Our neural circuit model could replicate the overall frequency of changes-of-mind from the experimental data (Figure 3a, right panel). The frequency of erroneous and correct changes-of-mind is similar to that of the experimental data at the 0.032 and 0.064 coherence levels, while the difference is more pronounced at intermediate-to-high coherence (0.128 and 0.256).

To investigate the relationship between changes-of-mind and choice accuracy more rigorously, we analysed choice accuracy as a function of coherence level in the presence and absence of changes-of-mind (Table 1, Figure 3b, left panel). In non-change-of-mind trials, accuracy increased with coherence ($b = 7.0$, $z = 4.6$, $p < 0.0001$, Table 1, Figure 3b, left panel), consistent with previous work on perceptual decision making [18,19]. However, in change-of-mind trials, choice accuracy was on average lower than in non-change-of-mind trials ($b = -1.0$, $z = -4.1$, $p < 0.0001$, Table 1, Figure 3b, left panel). Moreover, at intermediate-to-high coherence levels, the accuracy of changes-of-mind was above chance level ($p = 0.015$ for 0.128 coherence, $p = 0.001$ for 0.256 coherence, see also Figure 3b), demonstrating that these changes-of-mind were beneficial to the overall performance, i.e. they corrected an impending erroneous choice more often than introducing an error. Our neural circuit model readily accounted for these findings (Figure 3b, right panel). However, although there was an ascending trend for the rate of correct changes-of-mind with increasing coherence level, the trend was not as steep as that observed in the experiment.

Changes-of-mind are associated with slow decisions

Next, we analysed response times as a function of coherence level (Table 2, Figure 4a). In our fixed-duration task, the term "response time" refers to the time it took participants to initiate a movement towards one of the choice targets after stimulus offset (Figure 1a). For non-change-of-mind trials, mean response times followed the '<' pattern (Figure 4a, left panel), consistent with previous studies using the reaction-time

Fig 4. Changes-of-mind were most likely to occur in trials with prolonged initial response times. **(a)** Response times (z-scored within each participant; see Methods) for correct and error change-of-mind and non-change-of-mind trials from the experimental (left) and model (right). The '<' pattern of response times in the case of non-change-of-mind trials was consistent with previous observations [4, 18]. However, there was no difference between correct and error response times in change-of-mind trials, with a more pronounced pattern found in the model (correct and error change-of-mind data overlap in the right panel). Error bars indicate standard error of mean. **(b)** Probability of CoM as a function of coherence level grouped by the tertile of the initial response time for the experimental data (left panel) and the model (right panel). The majority of experimental change-of-mind trials occurred when response times were longest. The dominance of the third tertile in the model was more pronounced. Data for the first and second tertile overlap. Error bars indicate binomial proportion standard error of mean.

Table 2. Parameters of a linear mixed-effects model analysing response time as a function of coherence and choice correctness. The model included random intercept and random slopes for coherence, correctness, and their interaction.

	Estimate	Std. Error	df	t value	Pr(>|t|)
Intercept	0.5213	0.1094	2.9822	4.7657	0.0178
Coherence	-0.1040	0.4185	2.9384	-0.2485	0.8201
Is correct	-0.1767	0.0386	2.9667	-4.5750	0.0201
Coherence by Is correct	-0.7757	0.1381	3.8177	-5.6154	0.0057

task [4, 18]. More specifically, in correct choices, response times decreased with coherence level, while for incorrect choices, there was no evidence that response times varied with coherence level (Figure 4a). However, in the case of change-of-mind trials, mean response times were prolonged (compared to non-change-of-mind trials) regardless of the outcome of the trial. Our neural circuit model could account for the response time pattern in the case of non-change-of-mind trials, as in our previous work [20, 25]. Interestingly, our model qualitatively accounts for the relationship between response times and coherence level in the case of change-of-mind trials. Specifically, the model's response times for change-of-mind trials were prolonged (compared to non-change-of-mind trials), and did not vary between correct and error trials (Figure 4a, right panel, dashed and solid grey lines overlap). This was due to the tight relationship between high uncertainty levels and changes-of-mind, as we shall demonstrate below.

To clarify the relationship between the formation of an initial decision (as reflected in response times) and the subsequent emergence of a change-of-mind, we analysed the probability of a change-of-mind as a function of coherence level and initial response time (Table 3, Figure 4b). Confirming the observation from Figure 3a, the frequency of changes-of-mind decreased with coherence ($b = -2.78$, $z = -4.5$, $p < 0.0001$). Crucially, changes-of-mind were more likely to occur in trials with a prolonged response time ($b = 1.4$, $z = 2.4$, $p = 0.02$, Figure 4b, left panel). This is in sharp contrast with previous studies that linked changes-of-mind to fast initial responses [4, 23]. This discrepancy could be attributed to the differences between the experimental tasks as discussed above, and therefore the potentially different mechanisms underlying changes-of-mind.

Importantly, our neural circuit model accounted for the observed positive relationship between response time and changes-of-mind (Figure 4b, right panel). In

Table 3. Parameters of a linear mixed-effects model analysing probability of a change-of-mind as a function of coherence and response time. The model included random intercept and random slope for response time.

	Estimate	Std. Error	z value	Pr(>|z|)
Intercept	-4.3238	0.6156	-7.0241	0.0000
Coherence	-2.7840	0.6161	-4.5186	0.0000
RT	1.4052	0.5945	2.3637	0.0181
Coherence by RT	2.5390	0.9415	2.6966	0.0070

particular, the model suggests that changes-of-mind occur exclusively in trials with long response times. The replication of this finding by our neural circuit model suggests not only that the mechanism underlying changes-of-mind in our experiment and model could be similar, but also that these mechanisms are different from other mechanisms that rely on post-decision evidence accumulation [4, 6]. In contrast, below we demonstrate that the eDDM does not readily account for change-of-mind behaviour in the absence of new post-decision evidence.

eDDM does not readily account for change-of-mind behaviour in the absence of new post-decision evidence

eDDM has been previously used to fit response times (and choice accuracy) from change-of-mind trials in reaction-time tasks [4, 6]. The eDDM suggested, consistent with the experimental data in such paradigms, that change-of-mind trials are most likely to occur during trials with faster response times (compared to non change-of-mind trials). From the perspective of a drift-diffusion model, this added urgency is more likely to lead to fast errors. Moreover, with lower boundaries in the post-decision stage, the majority of the initially-fast-error trials become later-correct change-of-mind trials. This explains how the majority of changes-of-mind correct impending errors while, at the same time, leading to fast initial responses. To gain further insight into this mechanism, we simulated the eDDM [4]. We used parameter values that are fitted to the data from Subject 'S' in that study.

As a validation of our implementation of the eDDM, we first analysed the probability of change-of-mind and reaction time results for Subject S (see Figs. 5a and 5b. We found that our results matched those of [4]. Next, in order to understand the relationship between initial response times and changes-of-mind, we analysed the probability of a change-of-mind as a function of coherence level and initial response time (Supplementary Fig. 3). According to eDDM(Supplementary Fig. 3), changes-of-mind occur in trials with short response-times across all coherence levels, although, changes-of-mind are slightly more likely to occur in trials with prolonged response times, at least for $c < 0.256$.

Importantly, we simulated the same model with one minor change. When the accumulation reaches the initial decision threshold, we turn off the integration of the stimulus signal (i.e. $kc + \mu_0$ is set to 0). With this change, the post-decision process would be driven solely by noise fluctuations. We found that the majority of changes-of-mind in this case were correct-to-error changes, with increasing frequency of changes-of-mind with coherence level (see Fig. 5c). Furthermore, the majority of change-of-mind trials during high coherence level had fast initial response times (see Fig. 5d). Below, we provide a plausible explanation of this relationship between response times and changes-of-mind. In particular, we shall indicate the importance of a neural circuit feedback control mechanism via the uncertainty monitoring neuronal population.

Fig 5. In eDDM, probability of change-of-mind increases with coherence level when turning off post-decision stimulus evidence accumulation. Response time **(a)** and probability of a change-of-mind (CoM) **(b)** as a function of coherence for the eDDM [4] without turning off the stimulus post-decision. Our implementation of the simulation replicates the results reported by [4] for subject S in their Figure 2 and Figure 3, respectively. **(c)** When the post-initiation process (PIP) is driven entirely by noise fluctuations, the majority of changes-of-mind are errors. **(d)** Especially at high coherence levels (i.e. > 0.256), the majority of changes-of-mind occur in trials with fast initial response times (i.e., the first RT tertile).

Fig 6. Model uncertainty is strongly associated with changes-of-mind. **(a)** Uncertainty as a function of coherence level split by the type of trial (i.e. change-of-mind vs. non-change-of-mind). Change-of-mind trials are associated with higher uncertainty levels compared to non-change-of-mind trials regardless of the coherence level (see Fig. 4a, where response times are predicted to be the same for change-of-mind trials regardless of the coherence level). **(b)** Probability of a change-of-mind as a function of coherence level split by the magnitude of uncertainty level (three tertiles). Changes-of-mind occur only in the highest uncertainty tertile. See Methods for uncertainty level quantification.

Model predicts a strong link between high decision uncertainty and slow changes-of-mind

To clarify the relationship between uncertainty and changes-of-mind in our model, we investigate the pairwise relationships among decision uncertainty, changes-of-mind, and response times (see Fig. 6).

First, we analysed the mean uncertainty level (see Methods) as a function of task difficulty (i.e. coherence level) separately for change-of-mind and non-change-of-mind trials (Figure 6a). On average, uncertainty levels are higher in the case of change-of-mind trials compared to non-change-of-mind trials (Figure 7, middle panel), regardless of the outcome of the trial (i.e. correct or error). This suggests that in our model, in trials with a change-of-mind, high uncertainty level played a role in increasing the competition between the activities of the sensorimotor neuronal populations. This was further evidenced upon sorting the simulated trials based on tertiles of decision uncertainty levels; the probability of a change-of-mind is highly dependent on the decision uncertainty level (Figure 6b). Hence, our model suggests that changes-of-mind are strongly associated with high decision uncertainty. This was also reflected in the increased competition between the sensorimotor neuronal populations (Figure 7).

Due to the transient nature of this attractor, upon its disappearance, the network is given the chance to make the choice once again. In cases where this choice is different from the initial one, a change-of-mind occurs. It should be noted that this transient nature of the central attractor is a direct result of the transient activity profile of the uncertainty monitoring population (Figure 7).

Overall, our model simulations were not only consistent with our experimental findings, but also provided a prediction that the link between changes-of-mind and long initial response times could be due to high levels of decision uncertainty. Taken together, these results suggest a tight relationship among decision uncertainty, initial

response times, and changes-of-mind.

Fig 7. Faster ramping up and higher magnitude of activity for the uncertainty-monitoring neuronal population during low coherence (i.e. difficult) and change-of-mind trials. Activity is averaged over 3168 and 5346 non-change-of-mind trials for 0.032 and 0.256 coherence levels, respectively (left panels), and 120 change-of-mind trials for 0.032 coherence level (right panels). Blue (orange) colours: left (right) neuronal population. In trials without a change-of-mind, the sensorimotor and hand neuronal populations representing the correct (rightward) choice ramp up faster and reach higher activations in the case of high (0.256) coherence level compared to trials with a low (0.032) coherence level. The activity level of the uncertainty-monitoring neuronal population however is greater in trials with low (0.032) coherence. In change-of-mind trials, high uncertainty levels lead to high competition between the left and right sensorimotor neuronal population (through equal feedback excitation). Right panel: Left neuronal population is initially "winning", with a reversal occurring late in the trial. In downstream neuronal populations (for motor output), the left neuronal population reaches choice target, but is eventually suppressed by the rising activity of the right neuronal population. Bottom panel: Model-generated trajectories in the x positional space (see Methods).

Discussion

Many important decisions we make require prolonged deliberations. Yet, even well-prepared and thoughtful decisions are occasionally accompanied by a change-of-mind that reverses the initial choice. While considered a hallmark of cognitive flexibility, the mechanism underlying change-of-mind behaviour remains elusive. Previous studies on perceptual decision making have proposed that changes-of-mind are primarily driven by the accumulation of additional noisy sensory evidence after the initial decision.

We demonstrate that changes-of-mind can occur even in the absence of additional evidence after the initial decision. Furthermore, these changes-of-mind are associated with slow initial decisions, unlike changes-of-mind that are associated with post-decision sensory evidence accumulation. The neural circuit model we propose provides insight into the dynamics of this behaviour, predicting that changes-of-mind in the absence of new post-decision evidence are associated with high levels of decision uncertainty.

In the vast majority of trials involving a change-of-mind, the participants initiated a motor response only after the entire stimulus viewing duration was completed (Supplementary Figure 2b). Moreover, more than 99% of the changes-of-mind occurred later than 450ms after the initial response, which is outside the hypothesised delayed information processing window [24]. This supports the notion that the changes-of-mind we observed are not associated with post-decision accumulation of delayed evidence or explicitly provided new information, as opposed to the previous studies [4, 6, 7, 9]. Despite the absence of new post-decision evidence, changes-of-mind improved the initial decisions in the trials with intermediate-to-high stimulus coherence (Figure 3b), which was also the case in previous studies [4, 6, 23]. However, in sharp contrast to these studies, we found a positive relationship between initial response times and subsequent changes-of-mind (Figure 4a). More specifically, changes-of-mind were most likely to occur in trials with prolonged response times (Figure 4b, left panel). Hypothetically, this relationship can arise when initial response times and the frequency of changes-of-mind are both associated with high decision uncertainty. Future experimental work can directly test this hypothesis by requiring participants to report

their confidence retrospectively [7] or in parallel with their choice [6, 26] using the fixed stimulus viewing duration paradigm employed in this study. In the absence of such confidence reports in our paradigm, here we take a complementary approach. In particular, we demonstrate that our mechanistic model of decision uncertainty and change-of-mind could account for our experimental findings.

In our mechanistic model of decision uncertainty and change-of-mind behaviour, decision uncertainty is continuously monitored by a top-down uncertainty-monitoring neuronal population. Importantly, through an excitatory feedback loop, decision uncertainty continuously affects the neuronal integration dynamics. The model could account for the observed experimental data, including motor output, choice accuracy, response times, frequency of changes-of-mind, and, importantly, the positive relationship between initial response times and subsequent changes-of-mind.

This model is a variant of the model developed in our previous work [20], which was inspired by the neurophysiological recordings from brain regions encoding decision confidence or, reciprocally, decision uncertainty [14, 17]. In this work, we have simplified the uncertainty-monitoring module of the model to reduce the number of model parameters. In addition to the similarity of the neural profile of our model's uncertainty-encoding population (Figure 7, middle panel) to existing recordings [14, 17], this simplified model accounts for the main characteristics of decision uncertainty [17, 21, 26] (see Supplementary Figures 2a and 2b).

Our model provides insights into the mechanism of changes-of-mind observed in our experiment. Unlike the extensions of the drift-diffusion model [4, 10, 11, 22] and previous attractor network models [27], our model does not rely solely on post-decisional sensory evidence accumulation to induce changes-of-mind. In particular, drift-diffusion-based models rely on continual evidence accumulation post-decision to account for changes-of-mind. Importantly, such models do not readily extend to situations where no additional post-decision evidence is available after the initial decision. In contrast, in our model, the final outcome of a trial is dynamically affected by decision uncertainty monitored during the stimulus presentation. In trials with high levels of uncertainty, strong excitatory feedback from the uncertainty-monitoring neuronal population leads to a delayed initial response, due to the high competition between sensorimotor populations (Figure 7, [20]). At the same time, this increased uncertainty could lead to a change-of-mind (Figure 6a, [20]). Through this mechanism, our neural circuit model accounted for the observed positive relationship between initial response time and changes-of-mind (Figure 4b, right panel). This finding was further supported by the analysis of the probability of a change-of-mind as a function of uncertainty level (Figure 6b). More specifically, our model predicted that in situations where no new stimulus-related evidence could be sampled after the initial decision, changes-of-mind are most likely to occur during trials with high levels of uncertainty. Future work could test this by providing neural recordings of brain regions that encode decision uncertainty [14, 17] during changes-of-mind in a fixed-duration perceptual discrimination task.

Overall, our work provides a computational framework that explains changes-of-mind in the absence of new post-decision evidence, from sensory integration to uncertainty monitoring and motor output, by mechanistically linking decision uncertainty and changes-of-mind. Taken together, our findings highlight the role of top-down metacognitive processes in changes-of-mind [7, 8, 13, 14].

Parameter	Value	Reference or remarks
τ_S	100ms	Adapted from [25]
τ_h	50ms	Adapted from [20]
a	270 (V nC)$^{-1}$	Adapted from [25]
b	108 Hz	Adapted from [25]
d	0.154 s	Adapted from [25]
I_0	0.3255 nA	Adapted from [25]
$J_{N,\,ii}$	0.248 nA	Modified from [25]
$J_{N,\,ij}$	0.0497 nA	Adapted from [25]
μ_0	30	Adapted from [25]
$J_{A,\,ext}$	0.00052 nA Hz^{-1}	Adapted from [25]
J_{mc0}	0.002	Adapted from [20]
$J_{N,LR}$	2	Adapted from [20]
$J_{N,RL}$	2	Adapted from [20]

Table 4. Table of model parameter values.

Methods and Materials

Participants

Four healthy adults (one male, three female, 29 to 44 years old) were recruited to participate in the experiment in exchange for a €30 gift voucher. All participants were right-handed, and had normal or corrected-to-normal vision. The study protocol was approved by National University of Ireland (NUI) Galway Research Ethics Committee.

Apparatus

Participants performed the task in a sitting position in front of a desktop computer. Their head was fixed at 80 cm distance from a 24 inch monitor (1920 by 1080 pixels) using a chin rest. Mouse cursor coordinates were sampled at 60 Hz during stimulus presentation and at 100 Hz on the response screen. Participants' eye movements were recorded using an eye-tracker, but were not analyzed. The stimulus presentation software was programmed in Python using PsychoPy [28] and PyGaze [29].

Task

Participants performed a perceptual decision-making task (Fig. 1a). Each trial started when a participant clicked the start button located at the bottom of the screen. After a random delay (uniformly distributed over 700-1000ms), the RDK was presented for fixed duration of 800 ms, followed by a screen with two response options. A participant then moved the mouse cursor from the bottom of the screen to one of the top corners and then clicked on a response area to indicate their choice. Immediately after that, the feedback (green circle for correct responses, red for incorrect) was presented for 300 ms, followed by a fixation cross for another 300 ms. Participants were instructed to respond as fast and accurately as possible.

Stimuli and procedure

The random dot kinematogram (RDK) algorithm proposed by [18] and [19] was used for stimulus presentation. The dots were presented in a 5° circular aperture. During each frame, 3 dots were displayed. The monitor used for stimulus presentation has a refresh rate of 60 Hz. This entails that the resulting dot density is 16.7 dots per deg^2 per sec.

The dot velocity was set to 5°/sec. Each trial, the direction of the stimulus was determined randomly. The probability for each dot to move coherently on a given frame was determined by the coherence parameter.

The experiment consisted of four sessions held on four different days during a calendar week. Each session included 600 trials, grouped into ten blocks of 60 trials. Each block contained 10 trials for each of the six coherence levels (0, 0.032, 0.064, 0.128, 0.256, 0.512), randomly shuffled. In total, each participant completed 2400 trials, 400 for each coherence level.

Data analysis

A trial was labeled as a changes-of-mind trial if a response trajectory extended for more than 100 pixels (in the x-direction) to the side of the screen with the unchosen option. In total, there were 279 such trials, after 36 trials with an even number of changes-of-mind were excluded from all analyses.

Response time was measured as the time between the stimulus offset and the response onset. Response onset was determined as the onset of the first hand movement resulting in a mouse cursor displacement greater than 100 pixels; therefore, small movements resulting, e.g., from hand tremor did not affect RT measurement. In trials where participants initiated the response before the stimulus offset, the response time was considered to be negative. Overall, 9.1% of all trials had negative response time, with 56% of all negative response times observed at the highest coherence (see Supplementary Figure 1b for the proportion of negative response time trials as a function of coherence). Among change-of-mind trials, there were only three trials (1%) with a negative response time.

For linear mixed-effects statistical models (Tables 1–3), `R` package `lme4` was used. In all models, random effects of participant were included to account for individual differences, with the maximum random effects structure permitting model convergence. For testing the hypothesis that changes-of-mind improve accuracy, the `R` implementation of the exact binomial test (`binom.test`) was used.

A reduced neural circuit model of uncertainty

We used a simplified version of our previous neural circuit model of decision uncertainty and change-of-mind [20], in which the dynamics of uncertainty-encoding is described using one neural population (i.e. dynamical variable). The modelling of the sensorimotor and motor (i.e. hand) populations was unchanged (see below). The dynamics of the uncertainty-encoding neural population:

$$\tau_{mc}\frac{dy_{HU}}{dt} = [J_{VHU}(H_i + H_j) - g]_+ - y_{HU} \tag{1}$$

where $[\ ]_+$ denotes a threshold-linear input-output function. Synaptic coupling constant between the uncertainty-encoding population and the sensorimotor neural populations is denoted by J_{VHU}. H_i and H_j denote the neuronal population firing rates of the sensorimotor populations. At the beginning of a trial, some top-down inhibition is activated (g = 1000 nA) and 600 ms after stimulus onset from. Further, g is reactivated (with a value of 3000 nA) when the activity of one of the sensorimotor neural populations reaches a threshold (37.5 Hz). The result is a phasic activity response of the high uncertainty-encoding population that is reminiscent of recent neural recordings from the prefrontal cortex and medial frontal cortex during error correction post-decisional accumulation [7, 14, 17].

Uncertainty level quantification

Similar to our previous work [20], we used the maximum firing rate value of the uncertainty neuronal as a decision uncertainty measurement. In the case of trial-averaged measurements, we calculated the trial-averaged and SEM of these maximal values for each coherence level. We then normalised these values using simple scaling to bring them in the range of $[0, 1]$. This scaling can be described by:

$$X^{'} = \frac{X - X_{min}}{X_{max} - X_{min}} \tag{2}$$

Classifying model outputs and change-of-mind

Response time is recorded in the model as the moment the activity of one the sensorimotor populations reaches 37.5 Hz. In the simulation of the hand neuronal population, the target is fixed at 37.5 Hz. A simulated trial is classified as a change-of-mind if a reversal of dominance in firing rates between the two hand neuronal population occurs. A threshold of 2 Hz was used for the absolute difference in magnitude.

Mapping the activity of the hand neuronal populations onto the X positional space

To reproduce the typical trial dynamics observed in our experiment, we used a simple linear function to approximate the hand X position as a function of the neuronal firing rate [20]. This approximation can be described as follows:

$$x = q(y_{LH} - y_{RH}) \tag{3}$$

where q is some scaling factor. This scaling factor is determined as follows:

$$q = |C_{pos}|/H_{th} \tag{4}$$

where C_{pos} denotes the X position of the choice target (760px). H_{th} is the hand target threshold (37.5Hz).

Modelling the sensorimotor populations

Note: In all equations below, labels 1 and 2 denote being selective for rightward and leftward stimulus information, respectively.

We used a reduced spiking neural network model [30] described by two NMDA-mediated synaptic gating variables (i.e. dynamical variables) [25]. These two variables can be described by:

$$\frac{dS_1}{dt} = -\frac{S_1}{\tau_s} + (1 - \ S_1)\,\gamma H_1\,(x_1\ ,\ x_2) \tag{5}$$

$$\frac{dS_2}{dt} = -\frac{S_2}{\tau_s} + (1 - \ S_2)\,\gamma H_2\,(x_2\ ,\ x_1) \tag{6}$$

where:

γ: A constant

τ_S : The synaptic gating time constant.

H : A nonlinear input-output function (see below).

The firing rates of sensorimotor neuronal populations can be described by:

$$H_i = \frac{ax_i - b}{1 - e^{-d(ax_i - b)}} \tag{7}$$

$$x_i = J_{N,ii} S_i - J_{N,ij} S_j + I_0 + \ I_i + J_{mc0} y_{HU} \tag{8}$$

$$I_i = J_{A,ext}\ \mu_0 \left(1\ \pm \frac{\varepsilon}{100\%}\right) \tag{9}$$

where: a, b, d: Parameters for the input-output function fitted to a leaky integrate-and-fire neuronal model [30].

I_0: A constant denoting effective input bias.

c: Coherence level for a given trial.

$J_{N,\ ii}$ and $J_{N,\ ij}$: Synaptic recurrent connections strength.

I_i: Effective stimulus input do population i.

μ_0: The stimulus strength constant.

$J_{A,\ ext}$: External synaptic coupling strength.

J_{mc0}: The strength of the excitatory feedback from the uncertainty-encoding population.

Modelling the hand populations

We used a threshold linear function to model the action outputs via hand. We achieved persistent neural activity for the hand populations via mutual inhibition to create a line attractor model [31]. The dynamics of the two hand neuronal populations can be described by:

$$\tau_h \frac{dy_L}{dt} = [JH_1 - J_{N,LR}\, y_{HR} - g]_+ - y_{HL} \tag{10}$$

$$\tau_h \frac{dy_R}{dt} = [JH_2 - J_{N,LR}\, y_{HL} - g]_+ - y_{HR} \tag{11}$$

where:

$[\ ]_+$: Threshold-linear input-output function.

J: A coupling constant.

H_1 and H_2: Firing rates of the sensorimotor populations (see above).

$J_{N,LR}$: Synaptic coupling strength between left and right neuronal populations (i.e. effectively inhibitory connection).

g: Top-down inhibition (see Methods for more details).

Model simulation and analysis

The code to simulate the model (and analyse its outputs) was written in MATLAB. The code was tested against one version of MATLAB (2018a, on a Mac OS X workstation). The model parameters are summarised in Table 4. The model was simulated for 6000 trials per condition, using the same task specifications outlines above (i.e. 800ms fixed-duration). 3.4% of the trials were non-decision trials (i.e. target threshold was not reached) and were discarded. We used XPPAUT [32] for phase-plane analysis and parameter search. For within trial dynamics, we used a forward Euler-Maruyama numerical integration scheme. Integration time step set to 0.5ms. Smaller time steps did not affect our results.

Extended drift-diffusion model

In the eDDM, the dynamics of evidence accumulation can be described by:

$$dx = dt(kc + \mu_0) + \sqrt{dt}\sigma \tag{12}$$

where:

x: Dynamical (decision) variable.

c: Coherence level.

k, μ_0: Free parameters that control the speed-accuracy trade-off, set to 0.30 and 0.005, respectively.

σ: A random variable sampled from a normal distribution, i.e. $\sigma \sim \mathcal{N}(0, 1)$.

In the eDDM, the initial decision and decision time are determined by the threshold B (or $-B$) (which is set to 13.2 for Subject S). However, after the initial decision, evidence accumulation continues until threshold B_Δ is reached (which is set to 23.3 for Subject S) for confirmation of the initial decision or a change-of-mind. In particular, the post-decision accumulation process is driven by late-incoming evidence (and noise fluctuations), with a change-of-mind deadline of around 300ms.

Ethics statement

The study protocol was approved by NUI Galway Research Ethics Committee (ref: 15/DEC/02). All participants gave written consent to participate.

Supporting Information

S1. Fig.
(a) Response times for change-of-mind and non-change-of-mind trials and (b) number of trials with negative response time as a function of coherence level. In total, there were only three trials with a change-of-mind which had negative response time, one per each of three highest coherence levels.

S2. Fig.
(a) Uncertainty as a function of coherence level. '<' pattern: Uncertainty increases (decreases) with coherence level for error (correct) choices. Error bars indicate binomial proportion standard error of mean. (b) Response time as a function of uncertainty. Data points are collected from 36,000 trials. Strong correlation between uncertainty and response time (Pearson's r=0.74). Discarded trials with zero uncertainty.

S3. Fig.
Probability of change-of-mind as a function of coherence level grouped by tertile of the initial response time from the extended drift-diffusion model simulation for Subject S in [4]. Changes-of-mind occurred in trials with fast response times (tertiles 1 and 2).

Acknowledgments

This work was supported by Government of Ireland Postdoctoral Fellowship GOIPD/2015/481 (A.Z., D.O.H.). N.A. was supported by Ulster University Vice-Chancellor's Research Scholarship Award. K.W.-L. was supported by the National University of Ireland Galway Moore Institute Research Visiting Fellowship Award, the Northern Ireland Functional Brain Mapping Project 1303/101154803 funded by InvestNI

and the Ulster University, The Royal Society International Exchange Scheme under grant IE151293, and COST Action Open Multiscale Systems Medicine (OpenMultiMed) supported by COST (European Cooperation in Science and Technology).

Competing interests

The authors declare no competing interests.

Data availability

All codes and data needed to evaluate or reproduce the figures and analysis described in the paper are available online at: `https://osf.io/y385t/`. This includes the collected data, and the code for stimulus presentation, model simulation, and data analysis.

References

1. Gold JI, Shadlen MN. The neural basis of decision making. Annu Rev Neurosci. 2007;30:535–574.
2. Hanks TD, Summerfield C. Perceptual Decision Making in Rodents, Monkeys, and Humans. Neuron. 2017;93(1):15–31. doi:10.1016/j.neuron.2016.12.003.
3. Pouget A, Beck JM, Ma WJ, Latham PE. Probabilistic brains: knowns and unknowns. Nature Neuroscience. 2013;16(9):1170–1178. doi:10.1038/nn.3495.
4. Resulaj A, Kiani R, Wolpert DM, Shadlen MN. Changes of mind in decision-making. Nature. 2009;461(7261):263–266. doi:10.1038/nature08275.
5. Kiani R, Cueva CJ, Reppas JB, Newsome WT. Dynamics of neural population responses in prefrontal cortex indicate changes of mind on single trials. Current Biology. 2014;24(13):1542–1547. doi:10.1016/j.cub.2014.05.049.
6. Van Den Berg R, Anandalingam K, Zylberberg A, Kiani R, Shadlen MN, Wolpert DM. A common mechanism underlies changes of mind about decisions and confidence. eLife. 2016;5:e12192.
7. Fleming SM, van der Putten EJ, Daw ND. Neural mediators of changes of mind about perceptual decisions. Nature Neuroscience. 2018;doi:10.1038/s41593-018-0104-6.
8. Fleming SM, Daw ND. Self-evaluation of decision-making: A general Bayesian framework for metacognitive computation. Psychological Review. 2017;124(1):91–114. doi:10.1037/rev0000045.
9. Albantakis L, Branzi FM, Costa A, Deco G. A multiple-choice task with changes of mind. PLoS ONE. 2012;7(8). doi:10.1371/journal.pone.0043131.
10. Ratcliff R. A theory of memory retrieval. Psychological Review. 1978;85(2):59–108.
11. Ratcliff R, Van Zandt T, McKoon G. Connectionist and diffusion models of reaction time. Psychological Review. 1999;106(2):261.
12. Ratcliff R, Smith PL. A comparison of sequential sampling models for two-choice reaction time. Psychological review. 2004;111(2):333.

13. Fleming SM. Decision Making: Changing our minds about changes of mind. eLife. 2016;5:e14790.

14. Murphy PR, Robertson IH, Harty S, O'Connell RG. Neural evidence accumulation persists after choice to inform metacognitive judgments. eLife. 2015;4:e11946.

15. Del Cul A, Dehaene S, Reyes P, Bravo E, Slachevsky A. Causal role of prefrontal cortex in the threshold for access to consciousness. Brain. 2009;132(9):2531–2540.

16. Fleming SM, Weil RS, Nagy Z, Dolan RJ, Rees G. Relating introspective accuracy to individual differences in brain structure. Science. 2010;329(5998):1541–1543.

17. Kepecs A, Uchida N, Zariwala Ha, Mainen ZF. Neural correlates, computation and behavioural impact of decision confidence. Nature. 2008;455(7210):227–231. doi:10.1038/nature07200.

18. Shadlen M, Newsome W. Neural basis of a perceptual decision in the parietal cortex (area LIP) of the rhesus monkey. Journal of Neurophysiology. 2001;86(4):1916–1936.

19. Roitman JD, Shadlen MN. Response of neurons in the lateral intraparietal area during a combined visual discrimination reaction time task. Journal of Neuroscience. 2002;22(21):9475–9489.

20. Atiya NAA, Rañó I, Prasad G, Wong-Lin K. A neural circuit model of decision uncertainty and change-of-mind. Nature Communications. 2019;10(1):2287. doi:10.1038/s41467-019-10316-8.

21. Sanders JI, Hangya B, Kepecs A. Signatures of a Statistical Computation in the Human Sense of Confidence. Neuron. 2016;90(3):499–506. doi:10.1016/j.neuron.2016.03.025.

22. Pleskac TJ, Busemeyer JR. Two-stage dynamic signal detection: a theory of choice, decision time, and confidence. Psychological Review. 2010;117(3):864.

23. Albantakis L, Branzi FM, Costa A, Deco G. A multiple-choice task with changes of mind. PLoS ONE. 2012;7(8):e43131.

24. Gallivan JP, Chapman CS, Wolpert DM, Flanagan JR. Decision-making in sensorimotor control. Nature Reviews Neuroscience. 2018;19(9):519–534.

25. Wong KF, Wang XJ. A Recurrent network mechanism of time integration in perceptual decisions. Journal of Neuroscience. 2006;26(4):1314–1328. doi:10.1523/JNEUROSCI.3733-05.2006.

26. Kiani R, Corthell L, Shadlen MN. Choice certainty is informed by both evidence and decision time. Neuron. 2014;84(6):1329–1342.

27. Albantakis L, Deco G. Changes of mind in an attractor network of decision-making. PLoS Computational Biology. 2011;7(6). doi:10.1371/journal.pcbi.1002086.

28. Peirce JW. PsychoPy—psychophysics software in Python. Journal of Neuroscience Methods. 2007;162(1-2):8–13.

29. Dalmaijer ES, Mathôt S, der Stigchel S. PyGaze: An open-source, cross-platform toolbox for minimal-effort programming of eyetracking experiments. Behavior Research Methods. 2014;46(4):913–921.

30. Wang XJ. Probabilistic decision making by slow reverberation in cortical circuits. Neuron. 2002;36(5):955–968. doi:10.1016/S0896-6273(02)01092-9.

31. Gonçalves PJ, Arrenberg AB, Hablitzel B, Baier H, Machens CK. Optogenetic perturbations reveal the dynamics of an oculomotor integrator. Frontiers in Neural Circuits. 2014;8(February):1–22. doi:10.3389/fncir.2014.00010.

32. Ermentrout B. Phase plane: the dynamical systems tool. Pacific Grove, CA: Brooks/Cole. 1990;.

33. Grimaldi P, Lau H, Basso MA. There are things that we know that we know, and there are things that we do not know we do not know: Confidence in decision-making. Neuroscience & Biobehavioral Reviews. 2015;55:88–97.

34. Rabbitt P. Errors and error correction in choice-response tasks. Journal of Experimental Psychology. 1966;71(2):264.

35. Yeung N, Summerfield C. Metacognition in human decision-making: confidence and error monitoring. Philosophical Transactions of the Royal Society B: Biological Sciences. 2012;367(1594):1310–1321.

36. O'Connell RG, Shadlen MN, Wong-Lin K, Kelly SP. Bridging Neural and Computational Viewpoints on Perceptual Decision-Making. Trends in Neurosciences. 2018;doi:10.1016/j.tins.2018.06.005.

37. Wilson HR, Cowan JD. A mathematical theory of the functional dynamics of cortical and thalamic nervous tissue. Kybernetik. 1973;13(2):55–80. doi:10.1007/BF00288786.

38. Kiani R, Shadlen MN. Representation of confidence associated with a decision by neurons in the parietal cortex. Science. 2009;324(5928):759–764.

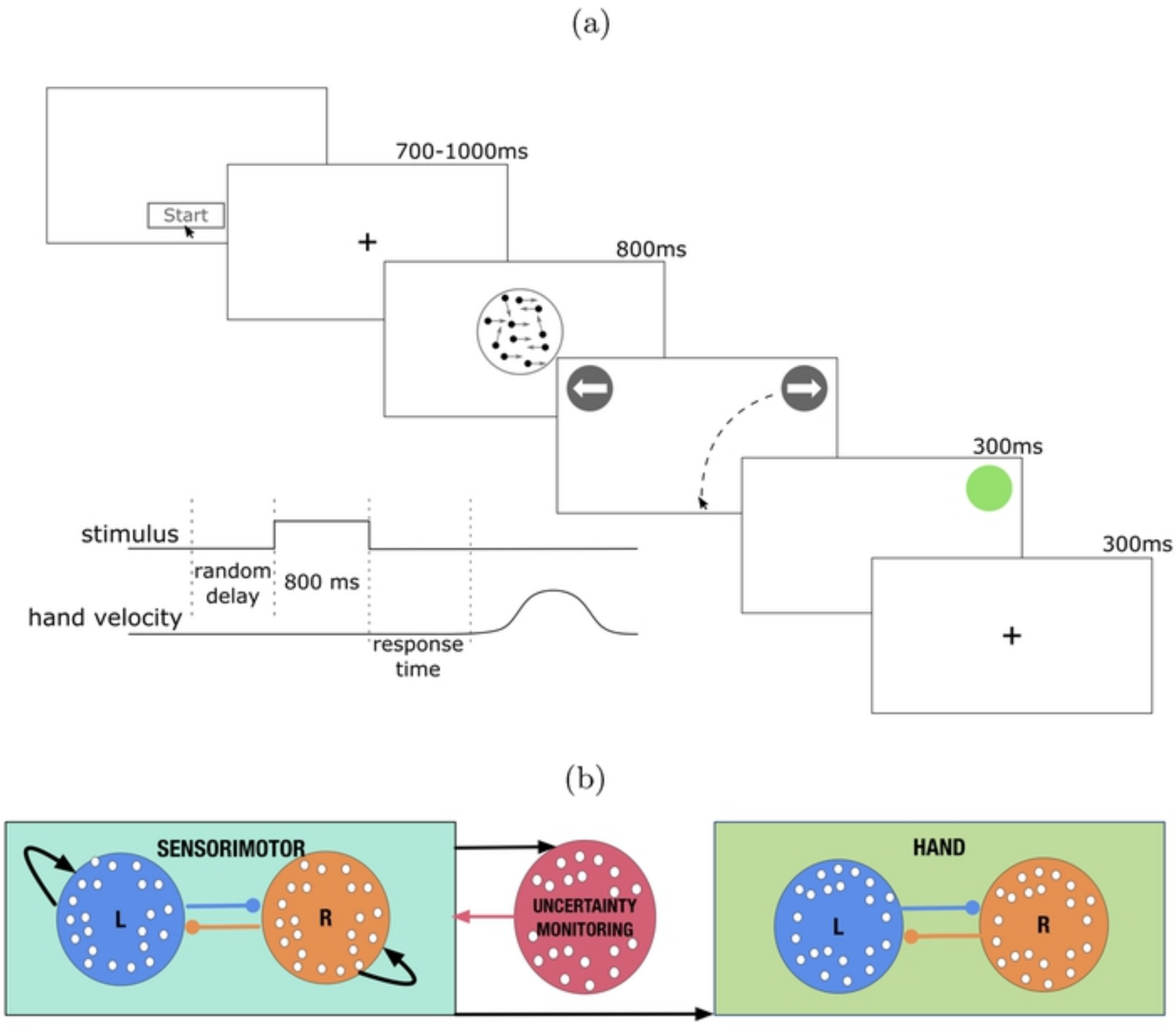
(a)
Start
700-1000ms
800ms
300ms
300ms
stimulus
random delay
800 ms
hand velocity
response time
(b)
SENSORIMOTOR
L
R
UNCERTAINTY MONITORING
HAND
L
R

Figure 1

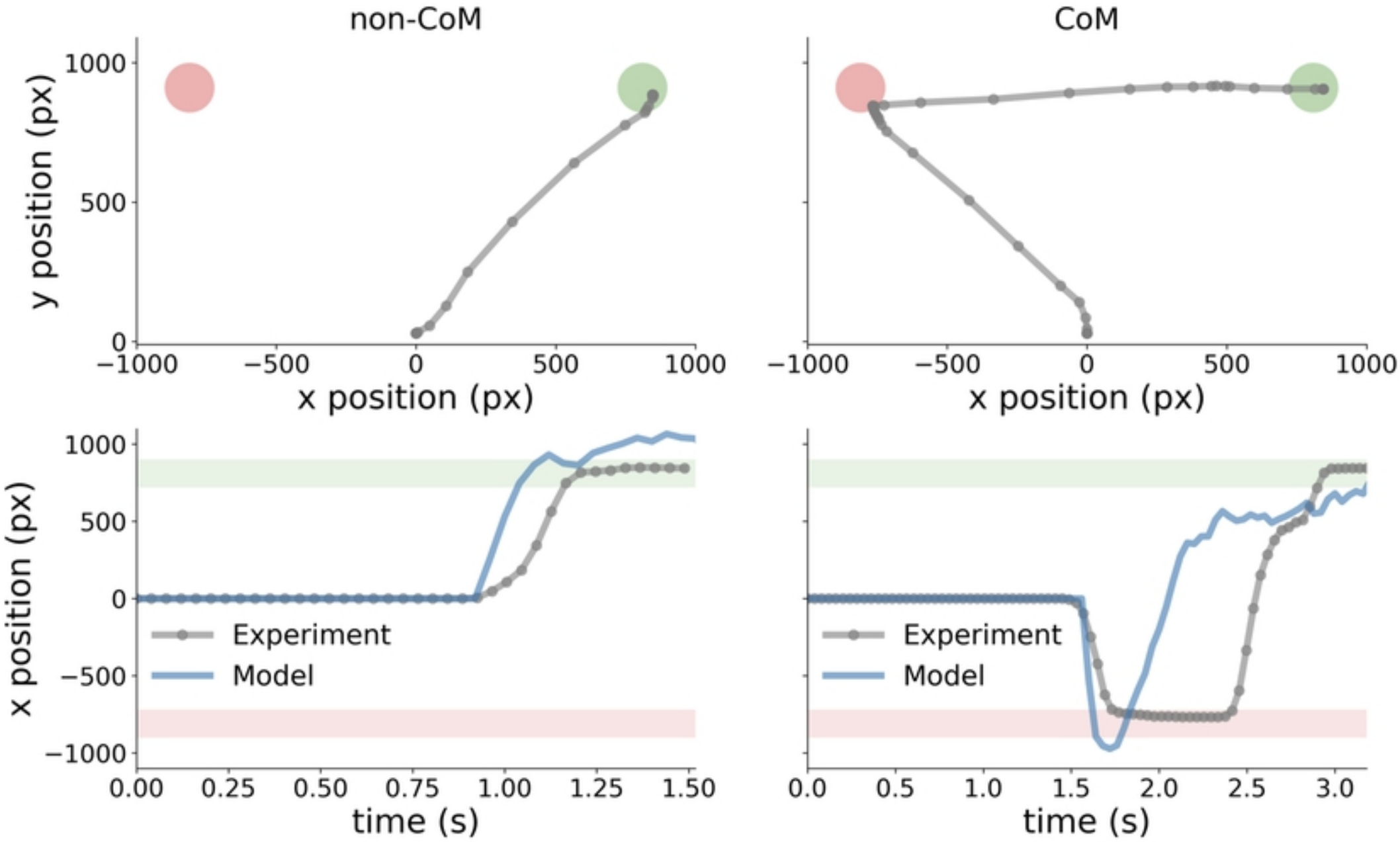
non-CoM
CoM
y position (px)
x position (px)
1000
500
0
−1000
−500
0
500
1000
x position (px)
time (s)
Experiment
Model
0.00
0.25
0.50
0.75
1.00
1.25
1.50
0.0
0.5
1.0
1.5
2.0
2.5
3.0

Figure 2

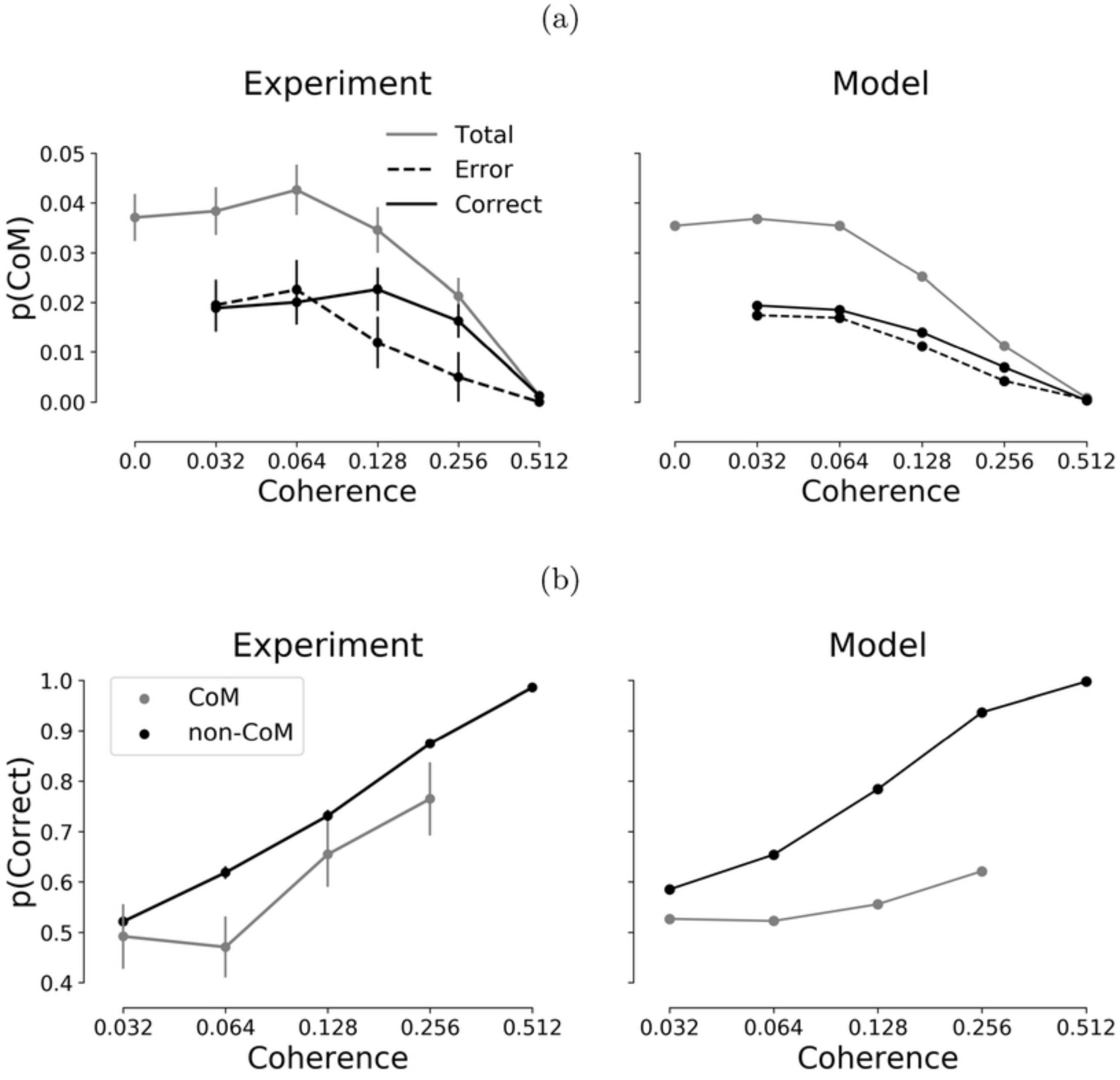
(a)
Experiment
Model
Total
Error
Correct
p(CoM)
0.05
0.04
0.03
0.02
0.01
0.00
0.0
0.032
0.064
0.128
0.256
0.512
Coherence
(b)
Experiment
Model
CoM
non-CoM
p(Correct)
1.0
0.9
0.8
0.7
0.6
0.5
0.4
0.032
0.064
0.128
0.256
0.512
Coherence

Figure 3

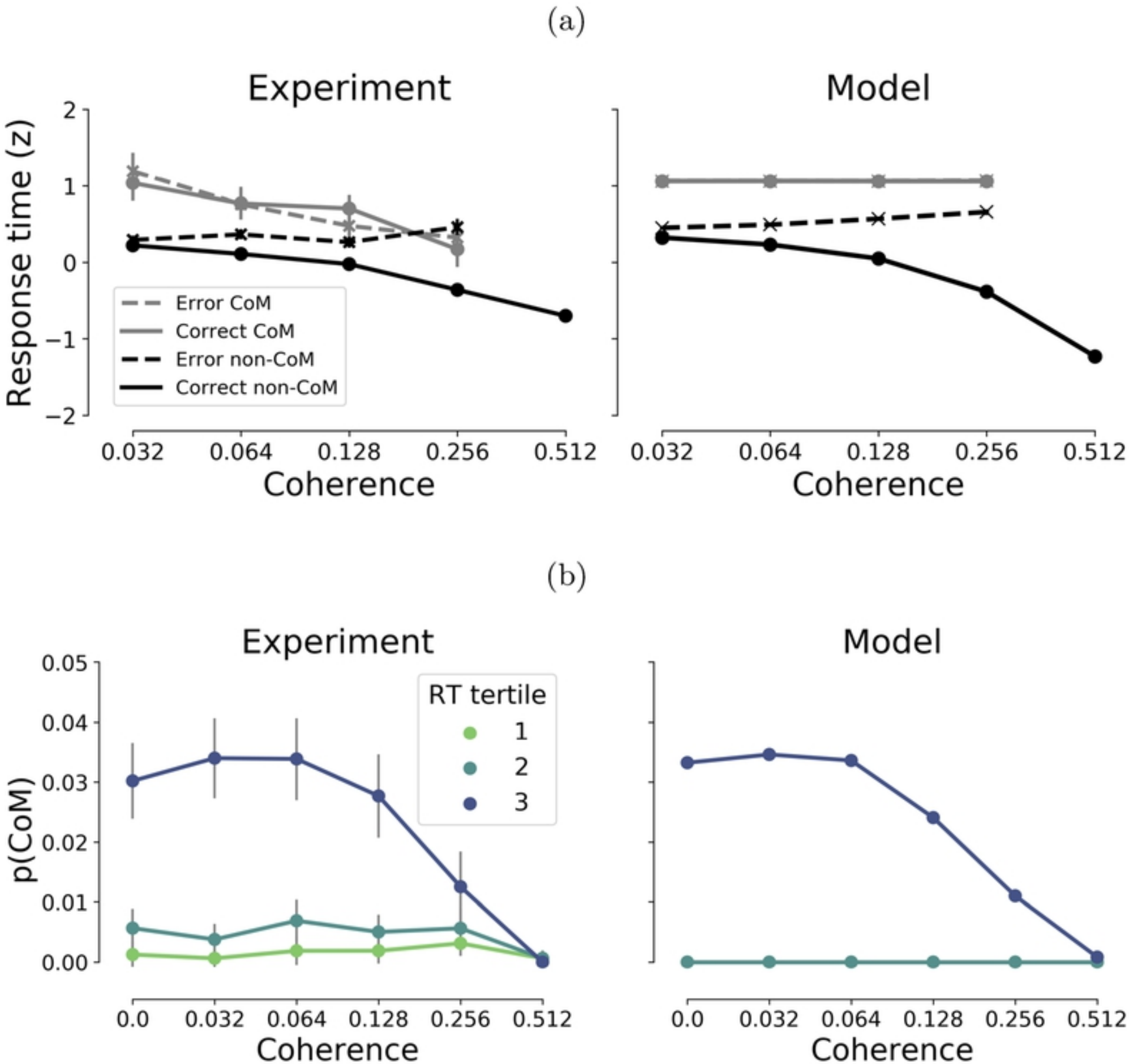
(a)
Experiment
Model
Response time (z)
2
1
0
−1
−2
Error CoM
Correct CoM
Error non-CoM
Correct non-CoM
0.032
0.064
0.128
0.256
0.512
Coherence
(b)
Experiment
Model
p(CoM)
0.05
0.04
0.03
0.02
0.01
0.00
RT tertile
1
2
3
0.0
0.032
0.064
0.128
0.256
0.512
Coherence

Figure 4

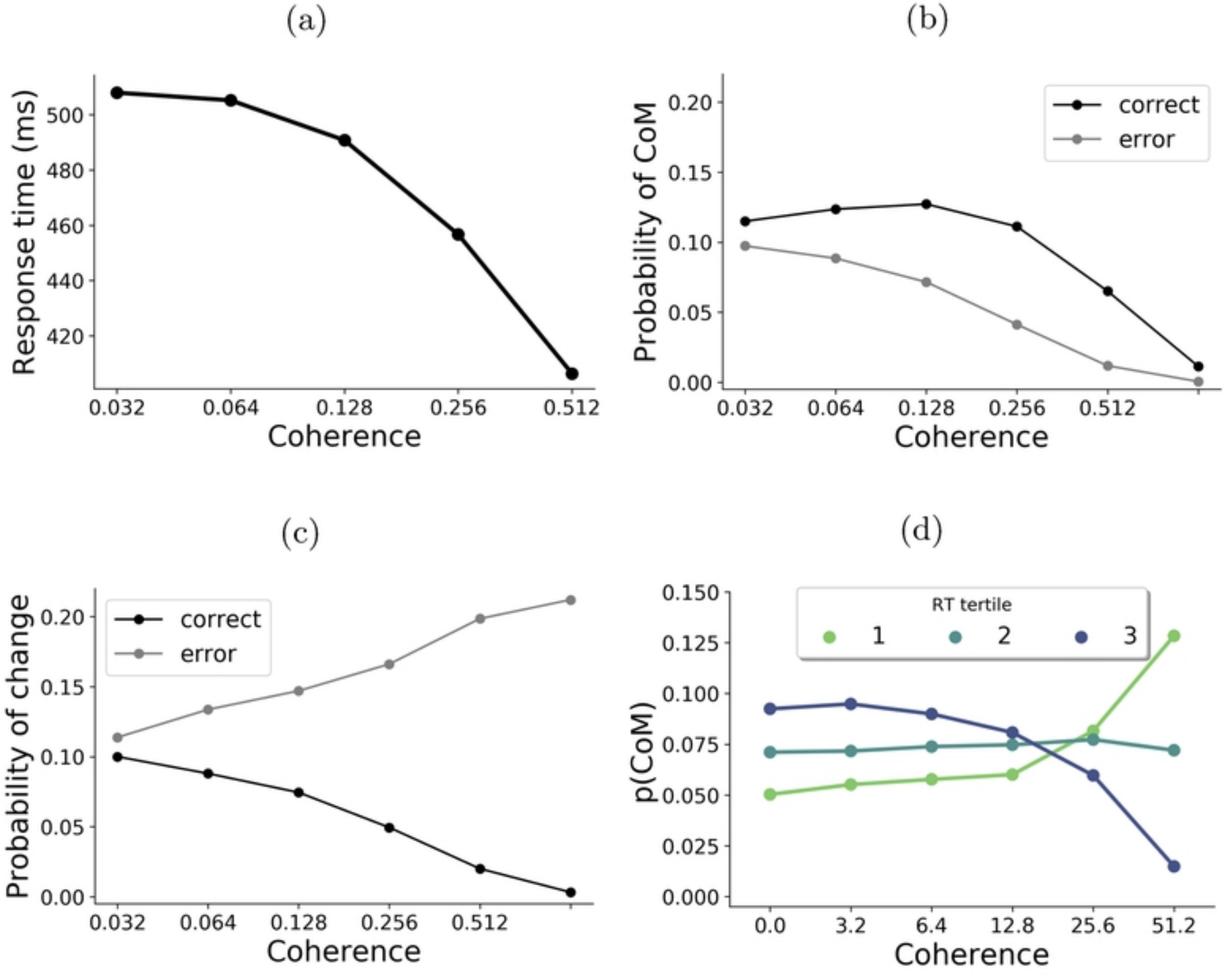
(a)
Response time (ms)
500
480
460
440
420
0.032
0.064
0.128
0.256
0.512
Coherence
(b)
Probability of CoM
0.20
0.15
0.10
0.05
0.00
correct
error
0.032
0.064
0.128
0.256
0.512
Coherence
(c)
Probability of change
0.20
0.15
0.10
0.05
0.00
correct
error
0.032
0.064
0.128
0.256
0.512
Coherence
(d)
p(CoM)
0.150
0.125
0.100
0.075
0.050
0.025
0.000
RT tertile
1
2
3
0.0
3.2
6.4
12.8
25.6
51.2
Coherence

Figure 5

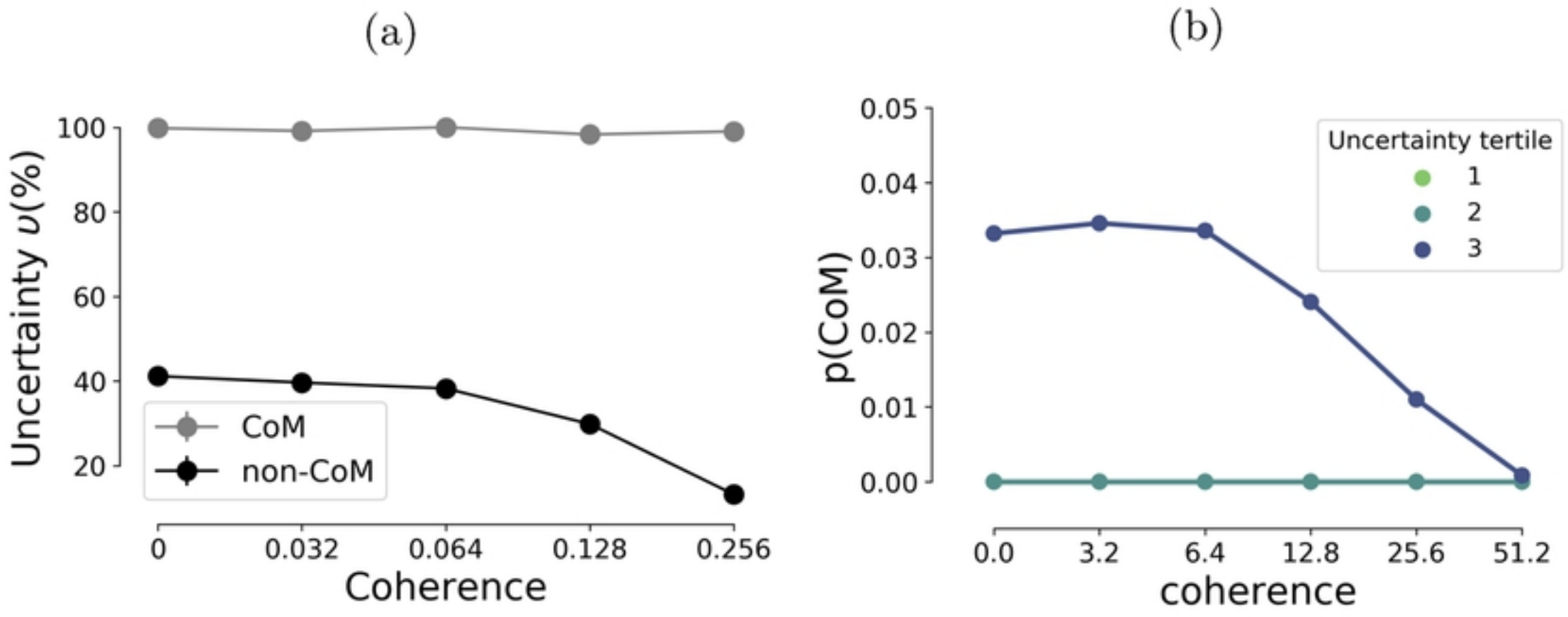
(a)
Uncertainty u(%)
100
80
60
40
20
CoM
non-CoM
0
0.032
0.064
0.128
0.256
Coherence
(b)
p(CoM)
0.05
0.04
0.03
0.02
0.01
0.00
Uncertainty tertile
1
2
3
0.0
3.2
6.4
12.8
25.6
51.2
coherence

Figure 6

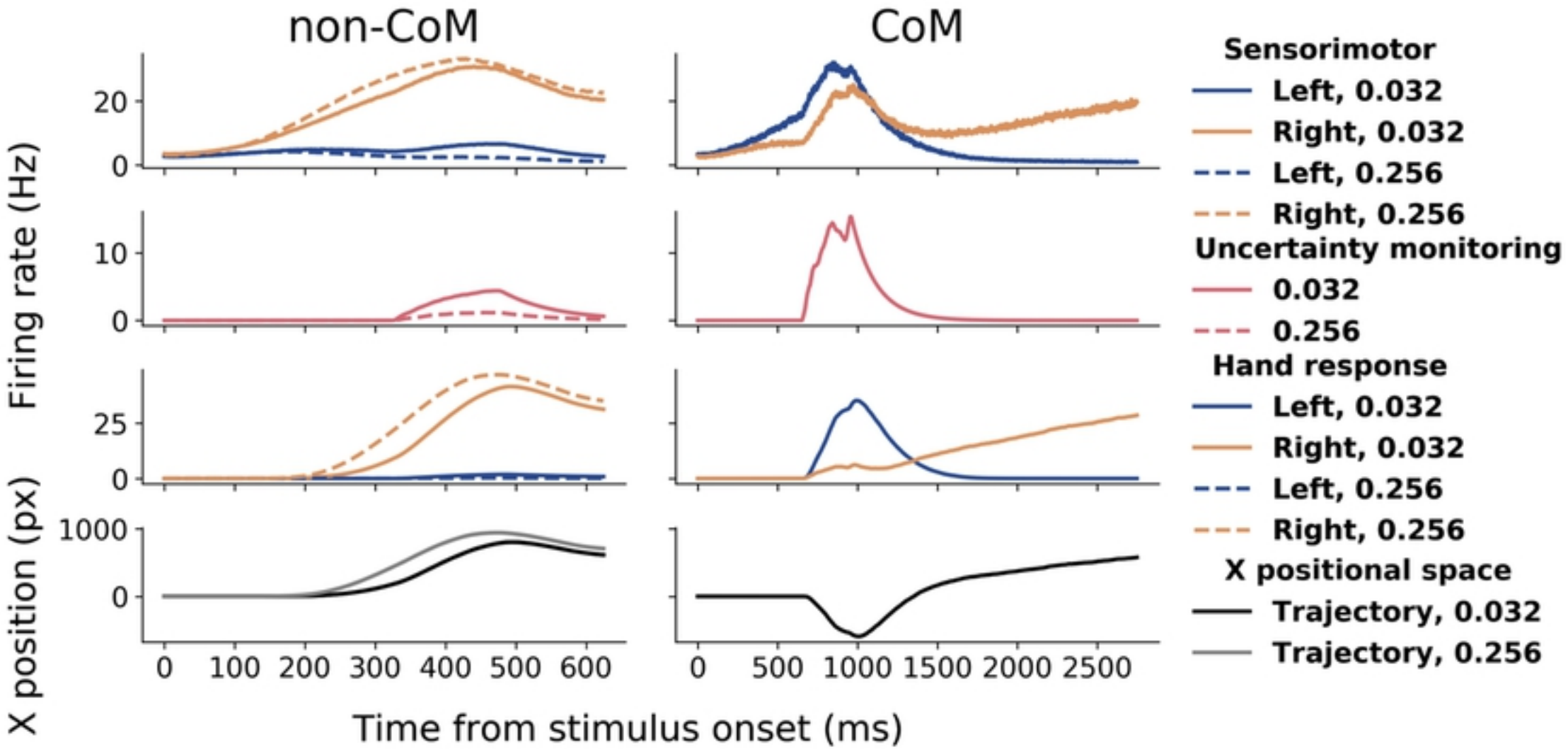
non-CoM
CoM
Firing rate (Hz)
X position (px)
Time from stimulus onset (ms)
Sensorimotor
Left, 0.032
Right, 0.032
Left, 0.256
Right, 0.256
Uncertainty monitoring
0.032
0.256
Hand response
Left, 0.032
Right, 0.032
Left, 0.256
Right, 0.256
X positional space
Trajectory, 0.032
Trajectory, 0.256

Figure 7